



OPEN

## Microwave assisted synthesis of fly ash based zeolites for degradation of reactive blue 19 dye from wastewater

Sanam Sadiq<sup>1</sup>, Shahzad Ali Shahid Chatha<sup>1</sup>✉, Shafaqat Ali<sup>2,3</sup>✉, Mudassar Shahid<sup>4</sup> & Pallab K. Sarker<sup>5</sup>✉

The current study presents the synthesis and characterization of corn stalk fly ash (CSFA) based zeolites using a microwave-assisted hydrothermal technique for the removal of reactive blue 19 dye from wastewater. Fly ash derived from the corn stalk was observed to belong to class "F" having low moisture and carbon levels. CSFA and synthesized zeolites were characterized by X-ray diffraction spectroscopy (XRD), energy dispersive x-rays (EDX)-scanning electron microscopy (SEM), and fourier-transform infrared spectroscopy (FTIR). The synthesized zeolites were found to have a large surface area and pore size which are suited best parameters for a potential adsorbent. The adsorption ability of the raw fly ash and synthesized zeolites was studied in batch experiments by varying different parameters such pH, dye concentration, contact duration, and adsorbent dose. It was observed that a pH of 8, an adsorbent dose of 2.10 g/100 mL, and a contact period of 40 min were the optimum parameters for the removal of reactive blue 19 dye up to 98.7%. It can be concluded that CSFA based zeolites are efficient adsorbent for the removal of reactive blue 19 dye from wastewater and may be an inexpensive and environmentally viable alternative material for wastewater treatment.

**Keywords** Corn stalk fly ash, Synthesis, Zeolites, Reactive blue 19 dye, Adsorption Isotherm

The unchecked industrialization, urbanization, and flattening trends in agricultural activities are drastically deteriorating the natural environment<sup>1</sup>. Among the numerous sources of pollution, comprising of nuclear reactors, oil refineries, different textiles and chemical based industries, automobiles, farmlands, townships and ecological heatwaves and landslides are contributing to deteriorate the environment up to various extents<sup>2</sup>. Due to heavily contaminated, unchecked and untreated industrial discharge, the air quality index is rising tremendously, alarming the life sustainability and on the other hand water pollution is emerging as challenging and intimidating issue around the globe<sup>3</sup>.

Consumption of coal and agricultural wastes (wood, sugar cane bagasse, corn stalk and rice husk) as cheap sources of energy is growing exponentially, leading towards the production of fly ash and bottom ash as solid waste at massive scale around the globe<sup>4</sup>. Fly ash is not only a waste but also an environmental vulnerability as particulate and leachate pollutant which also poses a financial liability for its safe disposal<sup>5</sup>. To meet the energy requirement around the world, the utilization of huge reservoir of coal and other raw fuel for the generation of electricity, the production of fly ash is expected to swell further<sup>4</sup>. Production and disposal of fly ash and bottom ash as solid waste posturing health and environmental threats all over the world. It is estimated that annual worldwide production of fly ash is approximately ranging up to 750 million tones/Anum<sup>6</sup>. Dumping this solid waste into landfill areas and inappropriate waste management behavior can be fatal for soil fertility and may have some detrimental effects by possible leakage of toxic heavy metals into ground water, puffing contaminants into the air as dust particulate and the catastrophic failure of burning residue as surface impoundments and disrupting ecological cycle<sup>7</sup>. One of the viable ways to reduce this heavy amount of solid waste is recycling it to some value-added product<sup>8</sup>. Fly ashes chemically composed of aluminosilicates and can be modified in

<sup>1</sup>Department of Chemistry, Government College University, Faisalabad 38000, Pakistan. <sup>2</sup>Department of Environmental Sciences, Government College University Faisalabad, Faisalabad 38000, Pakistan. <sup>3</sup>Department of Biological Sciences and Technology, China Medical University, Taichung 40402, Taiwan. <sup>4</sup>Department of Pharmaceutics, College of Pharmacy, King Saud University, 11451 Riyadh, Saudi Arabia. <sup>5</sup>Environmental Studies Department, University of California Santa Cruz, Santa Cruz, CA 95060, USA. ✉email: chatha222@gmail.com; shafaqataligill@yahoo.com; psarker@ucsc.edu

several ways to produce valuable zeolites for industrial applications like adsorption, catalysis for the removal of toxic heavy metals and other pollutants from wastewater<sup>3</sup>. Fly ash-based zeolites have also been reported for their applications in the field of health sciences, agricultural practices and animal feeds<sup>9,10</sup>. Zeolite can easily be synthesized by hydrothermal technique assisted by different modern approaches (microwave, sonication)<sup>11</sup>. Microwave assisted hydrothermal technique provides a short route and eliminates unwanted stages to develop zeolites with various morphologies<sup>12</sup>. Several scientists have designed and employed zeolite as an adsorbent to eliminate organic compounds from effluent, such as azo reactive dyes<sup>13</sup>.

A million tons of synthetic dyes are being produced worldwide for coloring various materials to develop colorful and attractive articles to compete with the modern marketing challenges<sup>4</sup>. Reactive dyes account for 60–70% of the total world production of synthetic dyes, used for coloring a variety of products, including leather, textiles, foodstuffs, and beauty products<sup>14</sup>. The heavy load of industrial effluents containing unexhausted/non-fixed reactive/synthetic dyes when discharged to waterbodies/ water system, pose severe medical risks to people<sup>15</sup> and devastate environments<sup>16</sup>. The presence of dyes in wastewater is a serious environmental concern that can affect human health drastically. Chemical as well as physical procedures including adsorption, deposition, flocculation, coagulation, and electrochemical degradation approaches are being employed to remove harmful azo dyes from industrial effluents/wastewater<sup>17</sup>. Generally, the wastewater treatment procedure must have some principal features for a sustainable process viz. cost effective, eco-friendly, and time saving<sup>5</sup>. Adsorption has seemed to be an economical, affordable, and easily manageable option for the elimination of dyes from wastewater<sup>18</sup>. Morphology, porosity and functionality are key features of good adsorbent that can aid in adsorption on surface of materials and scientists are conducting research to develop eco-friendly and sustainable materials derived from agricultural and industrial wastes as renewable feedstock<sup>19</sup>.

Fostering viable commercial and social development, scientists are looking for ways to protect the environment to guarantee a prosperous future through a sustainable green economy<sup>4</sup>. Investigation for innovative and multifunctional adsorbents owning the adsorption and catalytic attributes is the momentum of research to cope with the challenges of wastewater treatment<sup>20</sup>. Zeolites are reported to be multifunctional material with tremendous adsorption potential and catalytic properties to tackle the multi-polluted water<sup>5</sup>. In this context, corn stalk fly ash-based zeolites were synthesized using the microwave assisted hydrothermal approach to improve the functionality of material to be used as adsorbent for the removal reactive blue 19 (RB 19) dye from wastewater. Fly ash-based zeolite: A waste to value is not only a responsible way to manage solid industrial waste, but it can also serve as a functional mesoporous material for wastewater treatment containing dyes and heavy metals. The synthesized material is expected to find its way as a sustainable material to mitigate solid industrial waste and water pollution.

## Materials and methods

### Sampling of fly ash

The corn stalk fly ash (CSFA) was collected from local factories in Faisalabad, Pakistan. Fly ash samples were collected directly from the factory's emission control units with the assistance of boiler engineers. To account for variability in the composition of ash, multiple batches were collected over different shifts to ensure representative sampling<sup>21</sup>. The washing of collected ash was performed thoroughly with distilled water to eliminate soluble impurities and dried in oven at 150 °C. The dried ash then sieved with a standard mesh size to get fine particle size and stored in air tight containers<sup>22</sup>.

### Chemicals and reagents

All the chemicals and reagents were purchased from certified companies and were used without further purification mainly comprising of sodium hydroxide (Merck), sodium aluminate (Sigma Aldrich), hydrochloric acid (Sigma Aldrich), sodium acetate, (Sigma Aldrich), 2-propanol (Merck), ammonium acetate, (Sigma Aldrich), sodium silicate, (Merck), double distilled water (DD.H<sub>2</sub>O).

### Synthesis of microwave assisted Hydrothermal zeolites (MAHZ)

Hydrothermal process for zeolitization was performed according to the reported procedure with slight modification<sup>4</sup>. CSFA and 0.1 M of NaOH were mixed in a ratio of 1:1.67 in 20 mL of DD.H<sub>2</sub>O. And then sodium aluminate and sodium silicate (at a ratio of 0.4:1) were added to reaction solution. Subsequently, the mixture was crystallized for 30 min using microwave radiation using a self-adjusting microwave source (2.45 GHz, single mode, CEM corporation, USA). PTFE tube (28 mm ID X 108 mm) fitted with a complete reflux condenser mounted in microwave chamber. After decantation and centrifugation, the gel was filtered through a Gooch crucible using Whatman filter paper number No. 3. The volume of the supernatant was measured and kept in UHPE bottles for further analysis. The residue was rinsed five times with double distilled water (DD-H<sub>2</sub>O) to maintain a pH near 8. The gel was dried in an electric oven at around 80 °C for 8 h after rinsing the residues<sup>5</sup>. After drying, the synthesized product (MAHZ) was kept in a labeled airtight bag for its characterizations and applications (Fig. 1).

### Characterizations

The sorption behavior of ash sample and synthesized products were assessed using their cation exchange capacity (CEC), which is expressed in SI units as m.eq./100 g. Acetate method was used to determine the cation exchange capacity of residues<sup>23</sup>. The crystal structure was determined using XRD (Bruker D8 Advance) by exposing it to Cu-K $\alpha$  radiation. XRD analysis was carried out via contact angles of 10–50°, scanning at 0.02°. The SEM-EDX analysis was conducted to determine surface morphology<sup>24</sup>. The functional groups of the fly ash and products of this study were investigated using FTIR spectroscopy (with KBr pellets and analyzed using a Spectrum 65 of Perkin Elmer, USA)<sup>25</sup>. DTA and TGA (Diamond TG/DTA, Perkin Elmer, USA) set up was used to ascertain the

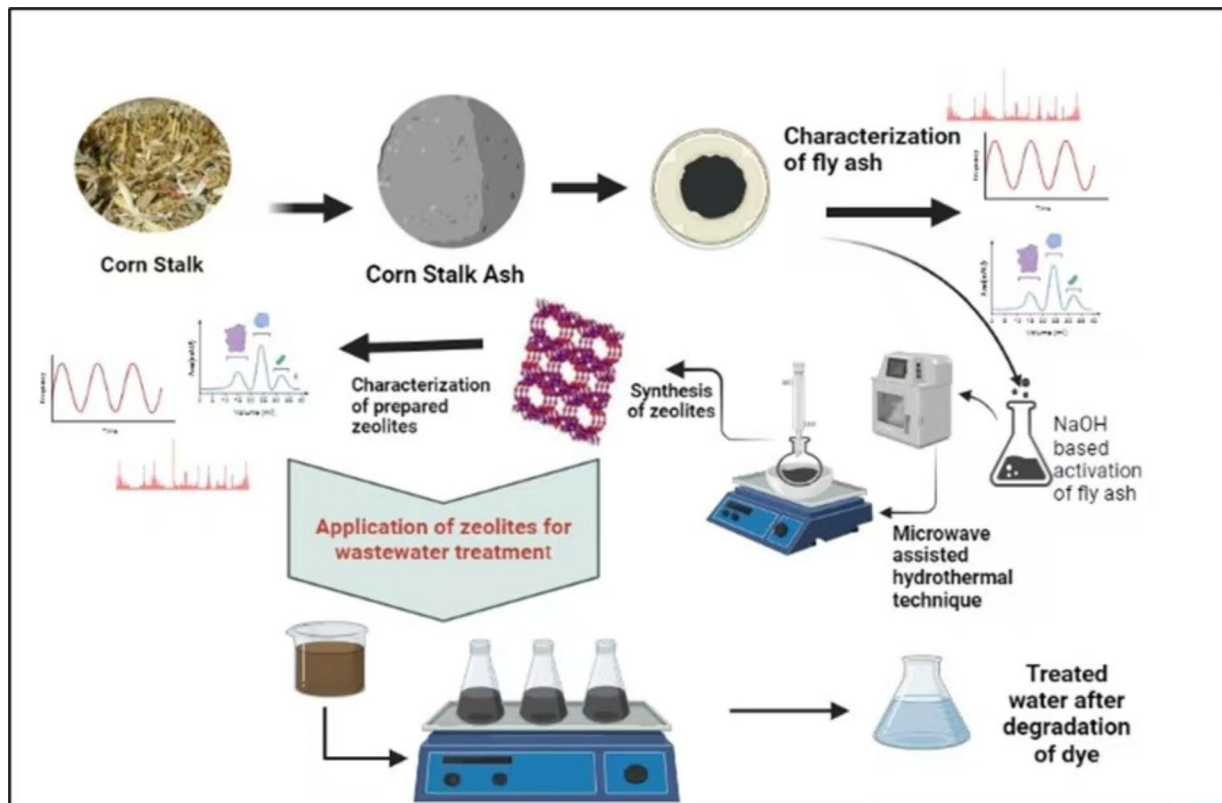


**Fig. 1.** Synthesis and application of microwave assisted hydrothermal zeolites.

thermal effects on CSFA and MAHZ<sup>26</sup>. An optical microscope and a CCD detector were used to collect Raman spectra excited with a 532 nm diode laser<sup>27</sup>. CHN Analyzer (Thermo Scientific TM, Waltham, MA, USA) was used to determine C, H, N, and S weight%ages<sup>28</sup>. Water leaching tests as described in ASTM D 3987-85 was performed on materials exposed to normal precipitation and Perkin Elmer 2280 model was used to measure the elemental concentrations in leachates using inductively coupled plasma-atomic emission spectroscopy<sup>29</sup>.

### Adsorption experiment

Batch experiments were conducted using CSFA and MAHZ as sorbent for investigating their dye (RB19) removal efficiency from synthetic wastewater. Several parameters, including pH (2–11), sorbent mass (0.3–2.10 g/100 ml), microwave irradiation time (0–70 min), and initial dye concentration (12.5–62.5 mg/L), studied at room temperature. A UV-VIS spectrophotometer (Lambda-25 by Perkin Elmer) with a wavelength of 663 nm was used to determine the uptake concentration of RB 19<sup>30</sup>. The following Equations were used to determine the percentage of dye removed and the amount of dye adsorbed.

$$\text{Dye removal (\%)} = \frac{C_i - C_t}{C_i} \times 100$$

$$q_e = \frac{(C_i - C_e)V}{W}$$

Here,  $C_i$ ,  $C_t$  and  $C_e$  represent initial concentration, concentration at any time 't' and concentration at equilibrium respectively. Whereas  $W$  is the mass of the adsorbent  $V$  represents volume of the solution in  $\text{g L}^{-1}$ .

## Results and discussion

### Characterization of CSFA and MAHZ

#### Physicochemical characterizations

Corn stalk fly ash (CSFA) predominantly consists of substantial volumes of silica ( $\text{SiO}_2$ , 40–60%) and alumina ( $\text{Al}_2\text{O}_3$ , 20–30%), along with lesser levels of other oxides like calcium oxide ( $\text{CaO}$ ), magnesium oxide ( $\text{MgO}$ ), and ferric oxide ( $\text{Fe}_2\text{O}_3$ ). The particle size of CSFA generally spans from 0.5  $\mu\text{m}$  to 300  $\mu\text{m}$ , facilitating advantageous reactivity and processability in synthesis. Synthesized zeolites showed several improved physicochemical properties relative to the original material. These zeolites consist of precisely structured crystalline aluminosilicate frameworks, recognized for their durability and consistency. A prominent elevated specific surface area, generally ranging from 200 to 400  $\text{m}^2/\text{g}$ . This is a significant improvement over the limited surface area of raw fly ash, typically ranging from 5 to 15  $\text{m}^2/\text{g}$ . The extensive surface area, together with the distinctive micro-

and mesoporous configurations of zeolites, facilitates exceptional adsorption and ion-exchange capabilities, rendering them optimal for water purification, gas separation, and catalysis. Another notable characteristic of synthesized zeolites was their CEC i.e. 200 to 400 meq/100 g. The higher CEC is attributed to the negative charge of the aluminosilicate framework, which facilitates ion exchange channels. The thermal stability of synthesized zeolites markedly exceeds that of raw fly ash, being stable up to 700 °C. This thermal stability makes them ideal for industrial procedures at high-temperature operations as described in Table 1.

The data from our synthesized zeolites shows significant consistency with existing literature<sup>31–33</sup> indicating the effectiveness of the technique used for synthesis and the raw material i.e. corn stalk fly ash.

#### FTIR analysis

The FTIR spectra of CSFA and MAHZ to elaborate their chemical bonding and functionalities are presented in Fig. 2a,b. The spectrum of CSFA shows a prominent peak at 644.57 cm<sup>-1</sup> indicates Si-O-Si bending vibrations, which are typically encountered in amorphous silica. The peak at 1606.23 cm<sup>-1</sup> indicates the bending vibrations of adsorbed water molecules (H-O-H), whereas the peak at 2855.82 cm<sup>-1</sup> shows C-H stretching vibrations, which are likely derived by leftover organic matter in the fly ash. These data demonstrate that the composition of CSFA is mainly constituted of siliceous particles, followed by adsorbed water and small organic components.

The FTIR spectrum of the MAHZ exhibits significant differences in comparison to CSFA, indicating the chemical and structural changes that happened during synthesis process. A prominent peak at 3384.17 cm<sup>-1</sup> is a strong representative of O-H stretching vibrations, underscoring the enhanced hydration of the zeolite structure. The peak at 1648.16 cm<sup>-1</sup>, showed strong H-O-H bending vibrations, is more prominent in MAHZ as compared to CSFA, shows enhanced water content of obtained zeolites. The peaks at 2363.81 cm<sup>-1</sup> indicates the presence of strong asymmetric stretching of CO<sub>2</sub> while peaks which appeared at 2830.66 cm<sup>-1</sup> represents the presence of C-H stretching vibrations. These characteristics illustrate that the hydrothermal treatment generates porous and hydrated properties in the synthetic zeolite. A comparison of the FTIR spectra reveals that the changes between CSFA and MHZA, indicating structural rearrangement and higher hydration in the zeolite. The presence of a prominent O-H stretching vibration at 3384.17 cm<sup>-1</sup> in MAHZ shows an established hydrated zeolite framework, while the transition of the silicate network of ash into crystal structure is attenuated by the presence of Si-O-Si bending vibration at 644.57 cm<sup>-1</sup> in CSFA and their absence in MAHZ. The stretching intensity of CSFA at 2855.82 cm<sup>-1</sup> and MAHZ at 2830.66 cm<sup>-1</sup> suggests decrease in C-H stretching vibrations and partial elimination of organic residues in the final product. The peak at 2363.81 cm<sup>-1</sup> indicates CO<sub>2</sub> absorbance ability of zeolites due to its excellent porosity and surface area and porosity. The structural and chemical changes seen in this study are validated by the synthesis of zeolites from CSFA which exhibits strong agreement with results published in the literature<sup>19,32,34</sup>.

#### Scanning electron microscopy (SEM)

SEM images of this study showed comprehensive morphological comparison of CSFA and synthesized zeolites. The irregularly shaped particles of fly ash with rough surfaces and heterogeneous distribution represents amorphous aluminosilicates in their raw condition. The SEM micrographs of CSFA and MAHZ of distinct magnifications i.e. 300 nm, 500 nm, 1 μm and 3 μm were used to illustrate the shape, structure, and grain size of the component minerals (Fig. 3). Carbon, silicon, calcium, magnesium, sodium, aluminum, sulfur, potassium, chlorine, and oxygen were quantified through EDX. In CSFA, the percentage of carbon weight was 87.11% which concludes that our separation approach worked well based on the CHNS analysis results. In contrast, MAHZ showed remarkable alteration, exhibiting clear crystalline structures, organized morphologies, and porous surface. These modifications indicated that the hydrothermal synthesis method was successful for the conversion of fly ash into zeolites. Table 2 elaborates the specifications analyzed by SEM graphics.

Zeolites synthesized in this study showed prominent resemblance with the characteristic of zeolitic materials documented in the literature<sup>12</sup>.

#### XRD analysis

Figure 4 presents the phase composition of both CSFA and MAHZ as determined by X-ray diffraction (XRD). The XRD patterns showed a remarkable change when fly ash turns into zeolite. This is shown by the fact that new crystalline peaks are shown up in the XRD spectra of zeolite frameworks. The CSFA spectrum has small, sharp peaks that show crystalline phases like quartz and mullite. It also has a big hump in the 20°–30° (2-theta) region, which showed an amorphous phase. On the other hand, the MAHZ spectrum exhibits distinct and strong diffraction peaks at specific 2-theta angles, suggesting the formation of a distinct crystalline structure associated with zeolite formation. The emergence of unique peaks in the MAHZ spectrum, exclusive to zeolite structures and not present in the CSFA spectrum, signifies the successful conversion of fly ash into zeolites.

| Parameter                                  | Fly Ash | Zeolite (Synthesized) |
|--|---------|-----------------------|
| SiO <sub>2</sub> content (%)               | 50–60   | 60–70                 |
| Al <sub>2</sub> O <sub>3</sub> content (%) | 20–30   | 25–35                 |
| Surface area (m <sup>2</sup> /g)           | 50–100  | 200–400               |
| CEC (meq/100 g)                            | < 50    | 200–400               |
| Thermal stability (°C)                     | < 500   | ~ 700                 |

**Table 1.** Physiochemical properties of CSFA and MAHZ.

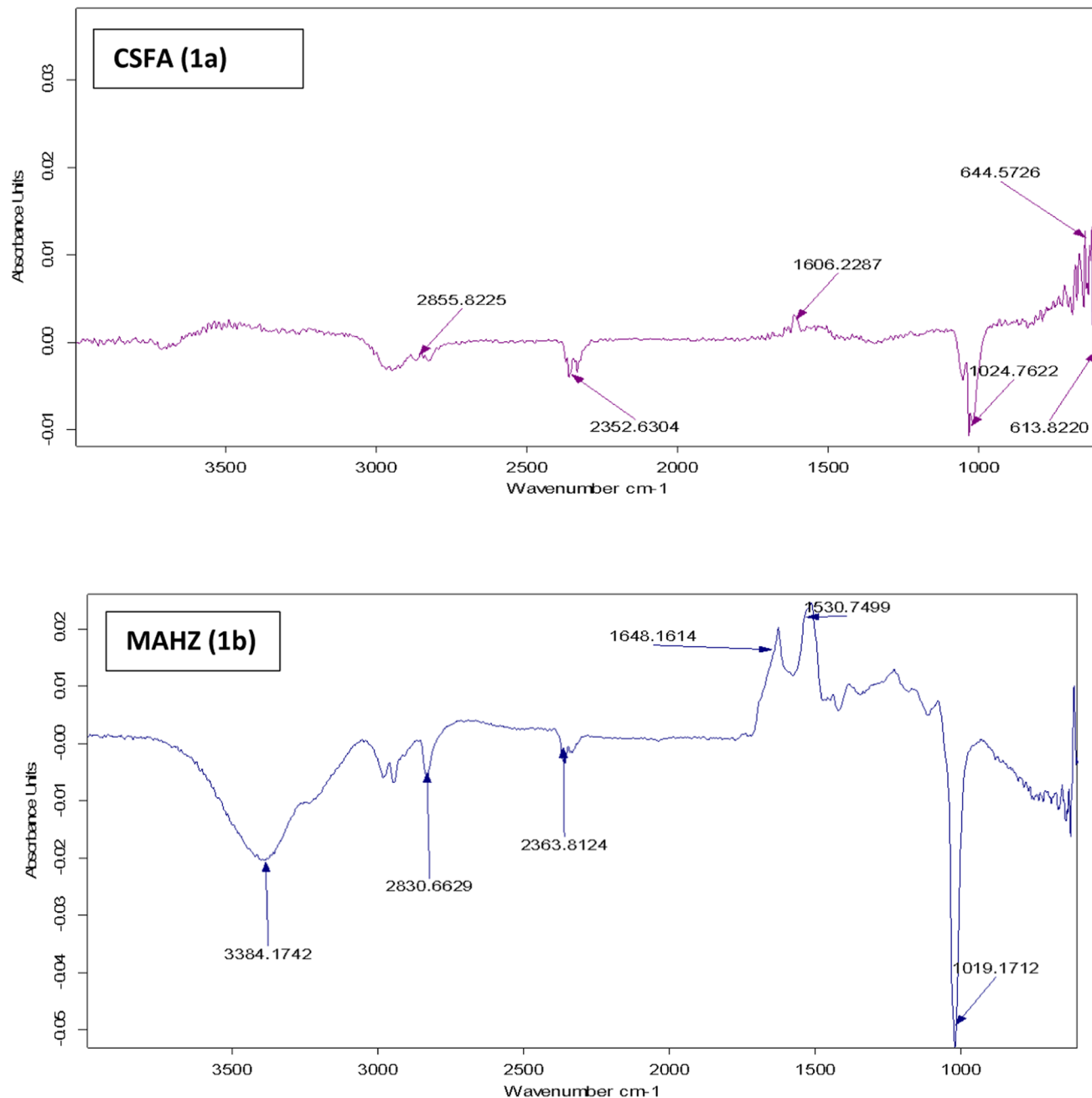


**Fig. 2.** FTIR spectra of (a) CSFA and (b) MAHZ.

The removal of peaks responsible for quartz and mullite during synthesis further supports the consumption of fly ash's first crystalline phases. The clear new peaks in the zeolite spectrum, which correspond to certain zeolite types reported in the established literature, demonstrated the production of a pure and crystalline zeolitic product<sup>7,35</sup>.

#### Raman analysis

Raman spectra of CSFA showed a wide, less defined spectral pattern, indicating heterogeneous, amorphous, and non-uniform phases. The amorphous form reduces the sharpness of the main peaks, which correspond to the silica and alumina structures. In contrast, MAHZ exhibits sharper and more distinct peaks, indicating the creation of a crystalline zeolite structure. Figure 5 illustrates this change in the spectral area, which includes Si-O and Al-O vibrations. The CSFA Raman spectra showed that the aluminosilicate phases are not ordered because of the large hump and scattered peak features. These characteristics developed into stronger peaks when converted to MAHZ, particularly in the 400–600  $\text{cm}^{-1}$  and 1000–1400  $\text{cm}^{-1}$  ranges. Zeolite frameworks usually have vibrations that are caused by the stretching of Si-O-Al bonds in tetrahedral units in both symmetric and asymmetric ways. The appearance of these peaks in MAHZ clearly demonstrated the structural reorganization

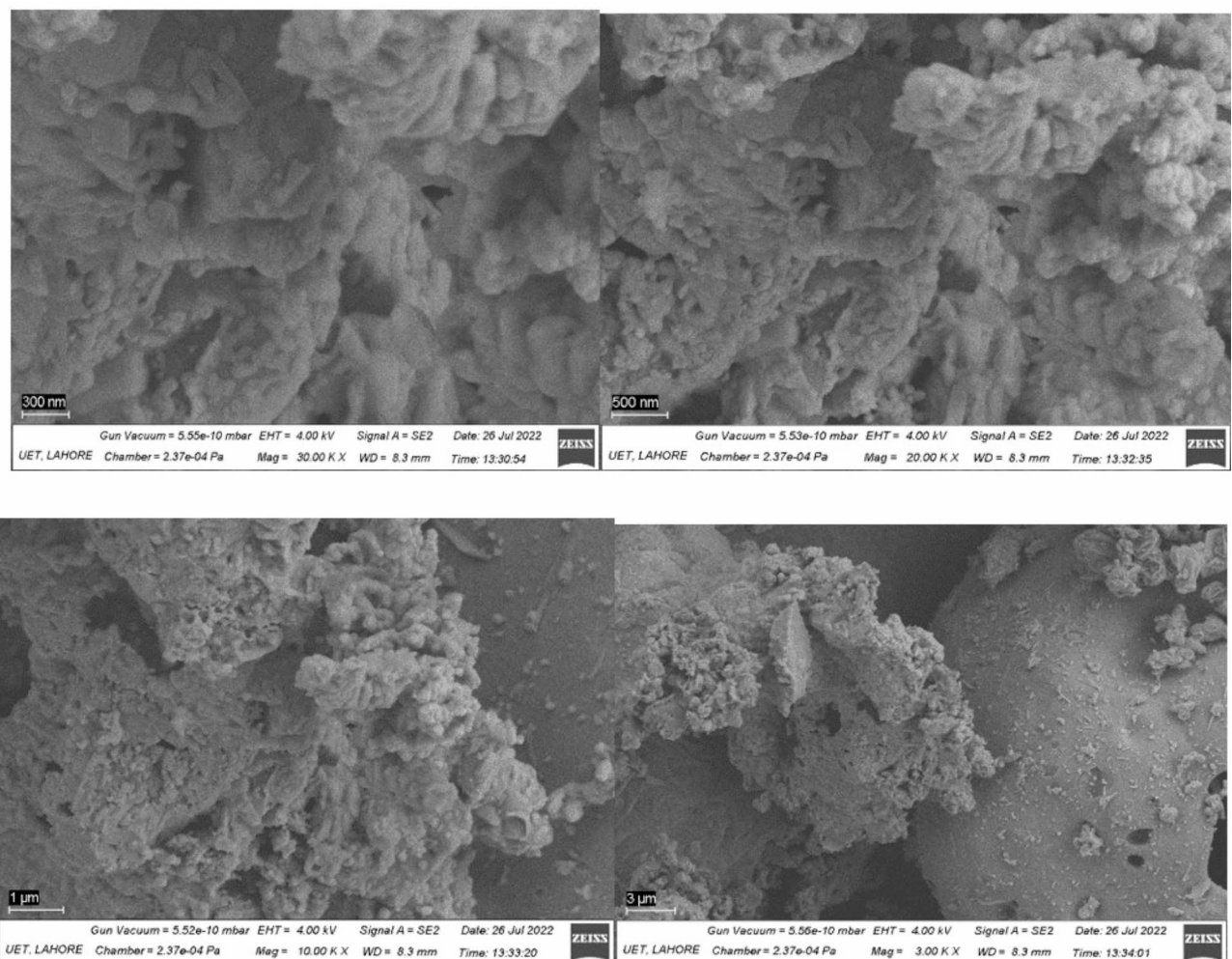


**Fig. 3.** SEM micrographs of CSFA and MAHZ. under different magnifications (300 nm, 500 nm, 1  $\mu$ m, 3  $\mu$ m).

| Specification              | CSFA                    | MAHZ                            |
|----------------------------|-------------------------|---------------------------------|
| Structure                  | Irregular and amorphous | Ordered and crystalline         |
| Surface morphology         | Rough                   | Uniform, porous features        |
| Particle size distribution | Heterogeneous           | Comparatively homogeneous       |
| Application potential      | Low                     | High (adsorption and catalysis) |

**Table 2.** Surface and structural comparison of CSFA and MAHZ.

of the aluminosilicates throughout the hydrothermal synthesis process, confirms the effective production of zeolitic frameworks. The main peak seen in MAHZ at around  $1100\text{--}1400\text{ cm}^{-3}$  is linked to the fact that zeolites have symmetric vibrations in silicate tetrahedra. The elimination of disordered vibrational patterns further supports the assertion that the fly ash underwent a phase transition into a crystalline substance with zeolitic characteristics. The recorded Raman spectra confirm the validity and repeatability of the fly ash-based zeolite synthesis, and the literature also supports the observed characteristics<sup>31,36</sup>.

#### Adsorption study

Zeolites are ideal material for adsorption of dyes and other pollutants from wastewater due to their large surface area, homogeneous micro porosity, and ion-exchange capacity which is clearly indicated by advance characterization approaches adopted in this work. MAHZ was used to remove RB 19 dye from aqueous solution using customized structural features to optimize the dye removal process.

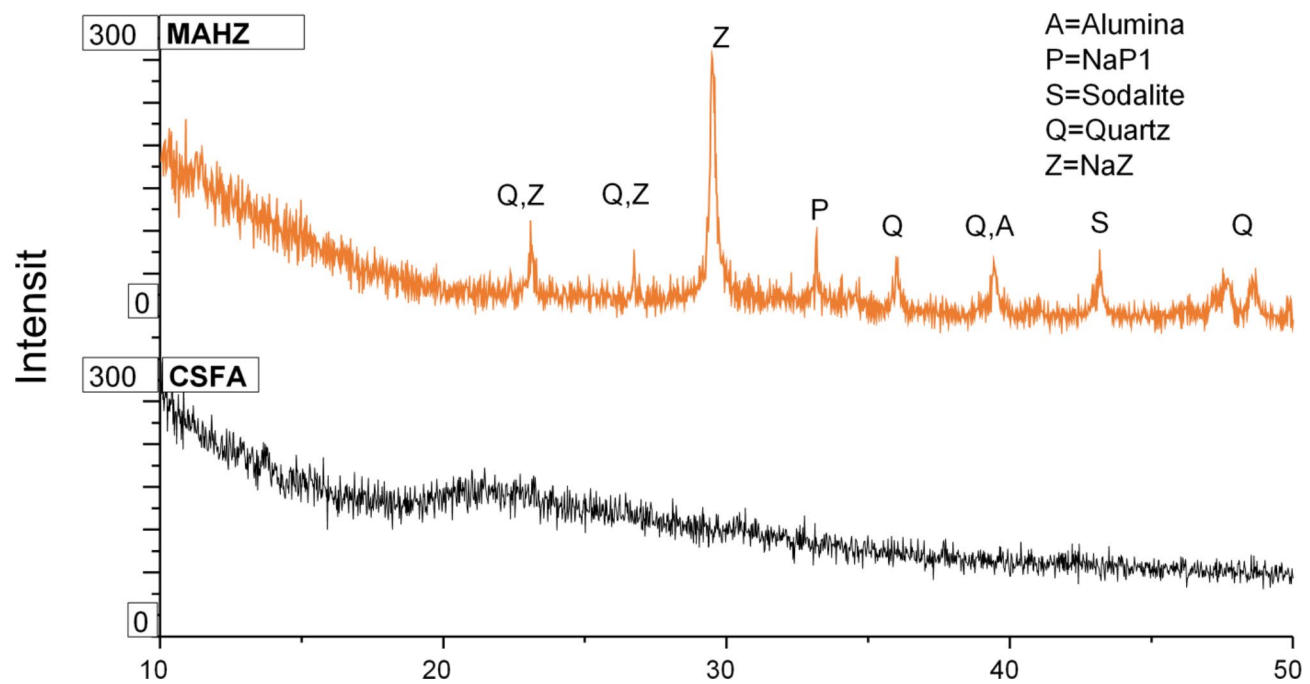


**Fig. 4.** XRD crystallogram of CSFA and MAHZ.

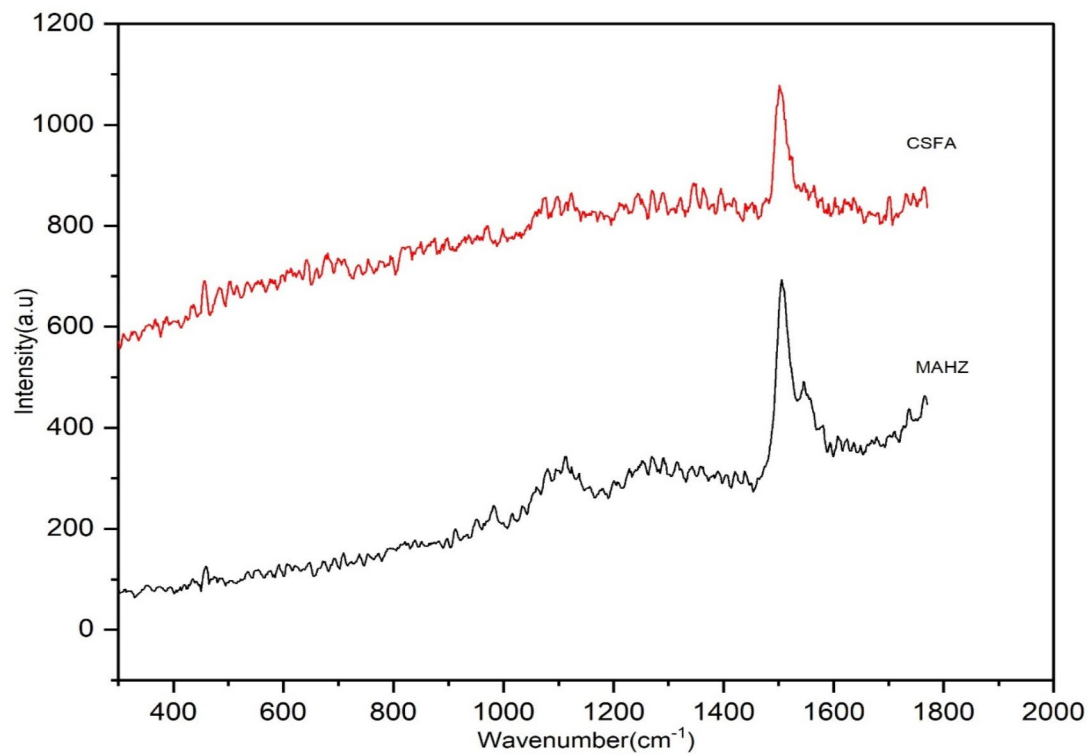


**Fig. 5.** Raman spectra of CSFA and MAHZ.

*Effect of pH*

The pH of a solution has a significant impact for the removal of dye from synthetic wastewater. pH can influence the surface charge of zeolite, the ionization state of the dye molecules, and finally the interactions between the zeolite and dye molecules. Therefore, the optimization of pH is essential for obtaining optimal adsorption and degradation efficiency of zeolites for dye molecules (Fig. 6). Previous studies have shown that altering the pH can increase electrostatic interactions, surface reactions, and the overall the efficiency of dye removal process<sup>37</sup>. At lower pH values (acidic circumstances), protonation causes the zeolite surface to become positively charged which can inhibit the adsorption of anionic dyes i.e. RB 19 due to electrostatic repulsion between the dye molecules and the positively charged surface. At higher pH levels (alkaline settings), the zeolite surface becomes negatively charged, hence can improve anionic dye adsorption through attractive electrostatic interactions between adsorbent and sorbate. Furthermore, degradation methods may vary with pH, since high pH stimulates the generation of hydroxyl radicals, which aids and facilitate the breakdown of dye molecules. According to findings of this experimental study which was conducted at various pH ranges (2–12) and keeping the other parameters constant, at pH 8, the zeolite surface has a balanced charge, allowing for strong electrostatic interactions with dye molecules while minimizing competition from hydroxide ions. Furthermore, breakdown efficiency is greater at pH 8 compared to highly acidic or strongly alkaline situations. The finding of this study are in line with the results presented in previous literature<sup>38</sup>.

*Effect of adsorbent dose*

The estimation of the number of active sites on adsorbent available for dye molecules to attach is determined by dosage that reflects its total adsorption capacity. Generally, the lower removal efficacy can be attributed to fewer active sites on adsorbent being accessible to dye molecules in the solution and vice versa. Therefore, the

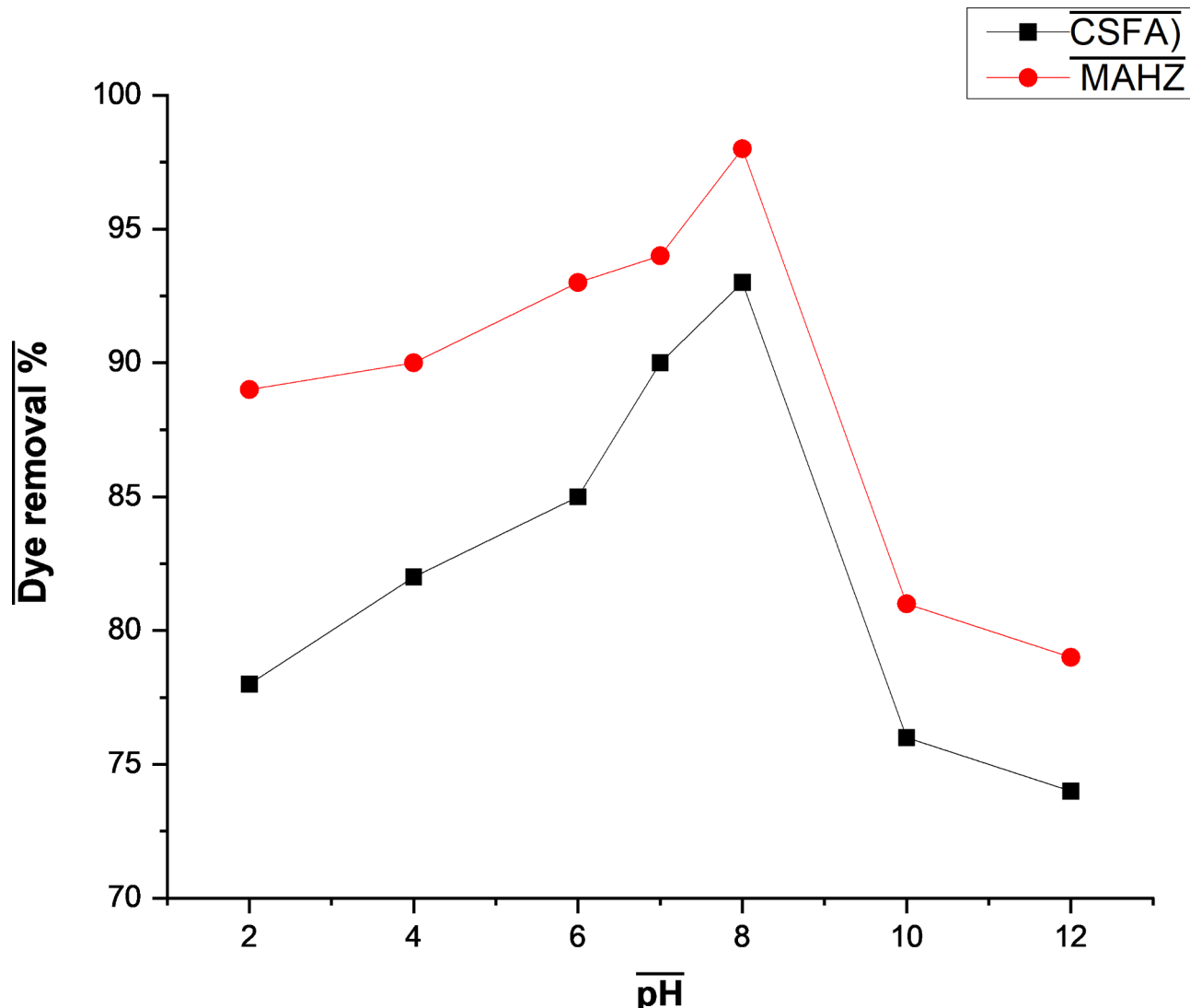


**Fig. 6.** Effect of pH on the removal efficiency of RB 19 dye at time 40 min, adsorbent dose: 2.10 g/100mL, initial dye concentration: 100ppm.

optimization of dose level of adsorbent is crucial. Generally, a higher dose results in more active sites that results in efficient adsorption process<sup>38,39</sup>. However, at a certain point, saturation of accessible sites and possible adsorbent particle aggregation, which can lower the effective surface area, may cause subsequent increases in adsorbent dose to provide little gains in dye removal efficiency<sup>39</sup>. In this study different adsorbent doses (0.5 g/100 mL to 3.0 g/100 mL) were examined in a series of batch adsorption experiments to find the most efficient quantity for eliminating RB 19 dye from synthetic wastewater (Fig. 7). The findings showed that dye removal efficiency improved by increasing the dose of adsorbent up to a certain point and then the rate of improvement levelled off. According to the findings of this study the adsorption capacity peaked at 2.10 g/100 mL adsorbent dose with more than 95% of the dye removal in a fair amount of time. The slight improvement in removal efficiency after this dosage indicates that the zeolite surface's active sites were adequately used at 2.10 g/100 mL. Since excessive adsorbent usage does not proportionately increase removal efficiency, this dose strikes a compromise between optimizing adsorption capacity and guaranteeing cost-effectiveness. The results demonstrate the potential of CSFA based zeolites as effective adsorbents for RB 19 dye removal which is fairly in close agreement / in line with the fundamentals of adsorption theory explained in the published literature<sup>39</sup>.

#### *Effect of time*

Contact time is the reaction duration required for maximum interaction between adsorbent and sorbate. Insufficient contact time may result in partial dye removal, while long reaction periods may be inefficient and costly for industrial applications<sup>39</sup>. Adsorption happens via electrostatic interactions, hydrogen bonding, and van der Waals forces, depending on the characteristics of the zeolite and dye molecules. In this study, the contact time was frequently varied to discover the most efficient period for dye removal. During the first 20 min of

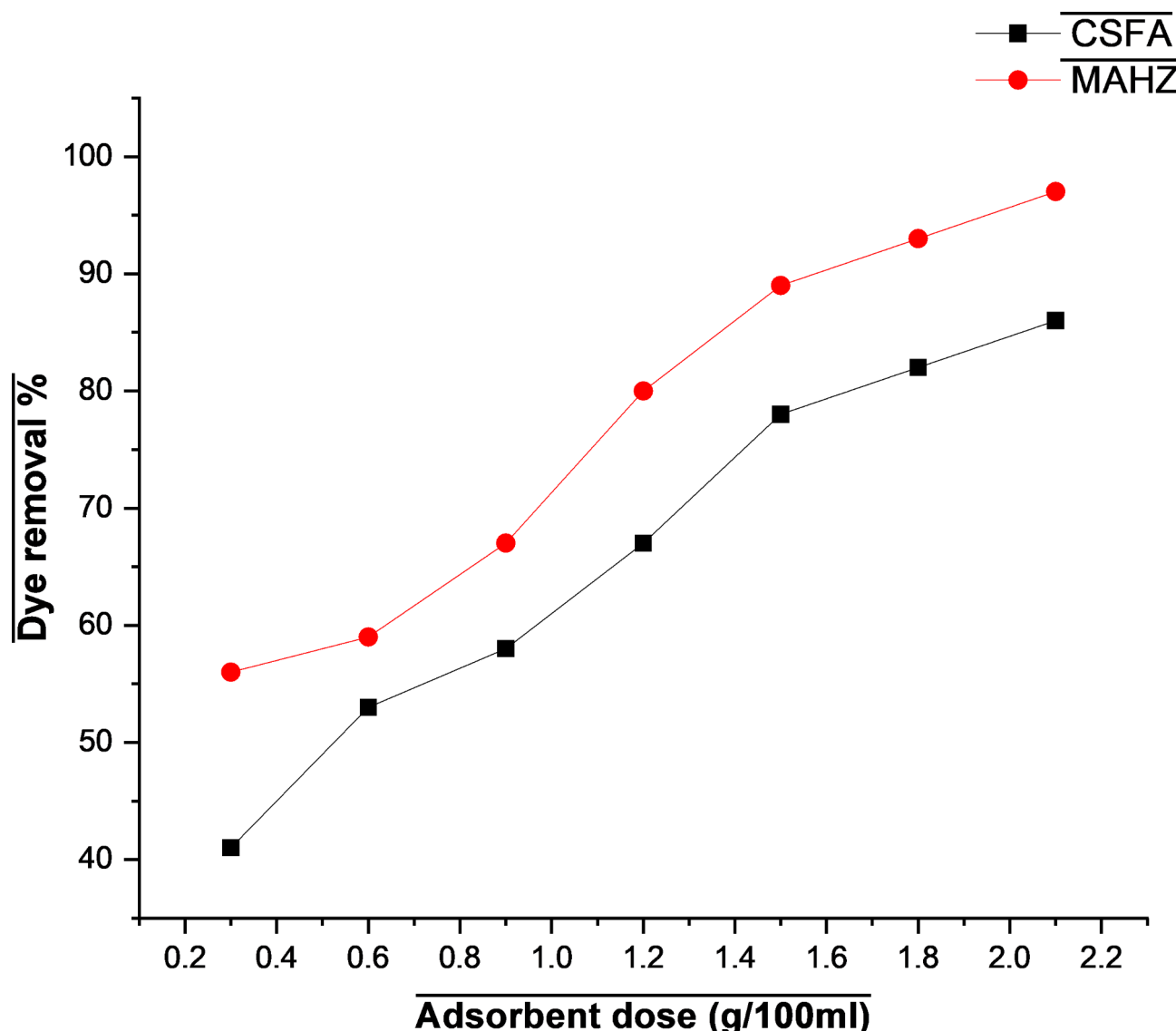


**Fig. 7.** Effect of adsorbent dose on the removal efficiency of RB 19 dye at time 40 min, pH = 8, initial dye concentration: 100 ppm.

contact it was observed that the adsorption of RB 19 was quick, which can be attributed to the abundance of active sites for adsorption on zeolites. Then during 20 to 40 min, the adsorption process slowed down as active sites on the zeolite surface were gradually occupied (Fig. 8). The dye molecules continue to interact with less accessible or weaker locations on the zeolite and hence the rate of adsorption slowed down and after 40 min, the adsorption process reaches a plateau, which indicated the establishment of equilibrium. At this point, the adsorption sites are practically saturated, and the driving force for mass transfer between the solution and the zeolite has greatly decreased. Additional reaction time yielded a non-significant improvement in dye removal efficiency which can affect the cost of process making it unfit for commercial applications. The dynamic trends and mechanism of adsorption process of this study was found fairly consistent with the previous investigation in this field<sup>40</sup>.

*Effect of initial dye concentration*

This study examined zeolite's adsorption ability for RB 19 and investigated how the initial dye concentration (IDC) affects adsorption effectiveness. The original concentration ( $C_0$ ) of dye in a solution is another factor that can affect the adsorption of RB 19 dye molecules. Figure 8 exhibits the impact of initial dye concentration on CSFA and MAHZ for removal / degradation (%) of RB 19. Keeping the pH 8.0 and temperature 25 °C, adsorbent (zeolites) dose 2.10 g/100L for 40 min constant experiments were conducted using initial dye (RB 19) concentration 50 to 300 mg/L. These findings revealed that although the adsorption capacity rises with increasing dye concentrations, until the zeolite's active sites become saturated, resulting in a drop in the percent removal of RB 19. Figure 9 clearly demonstrates that at higher IDC the removal efficiency was maximum (98.7%). To

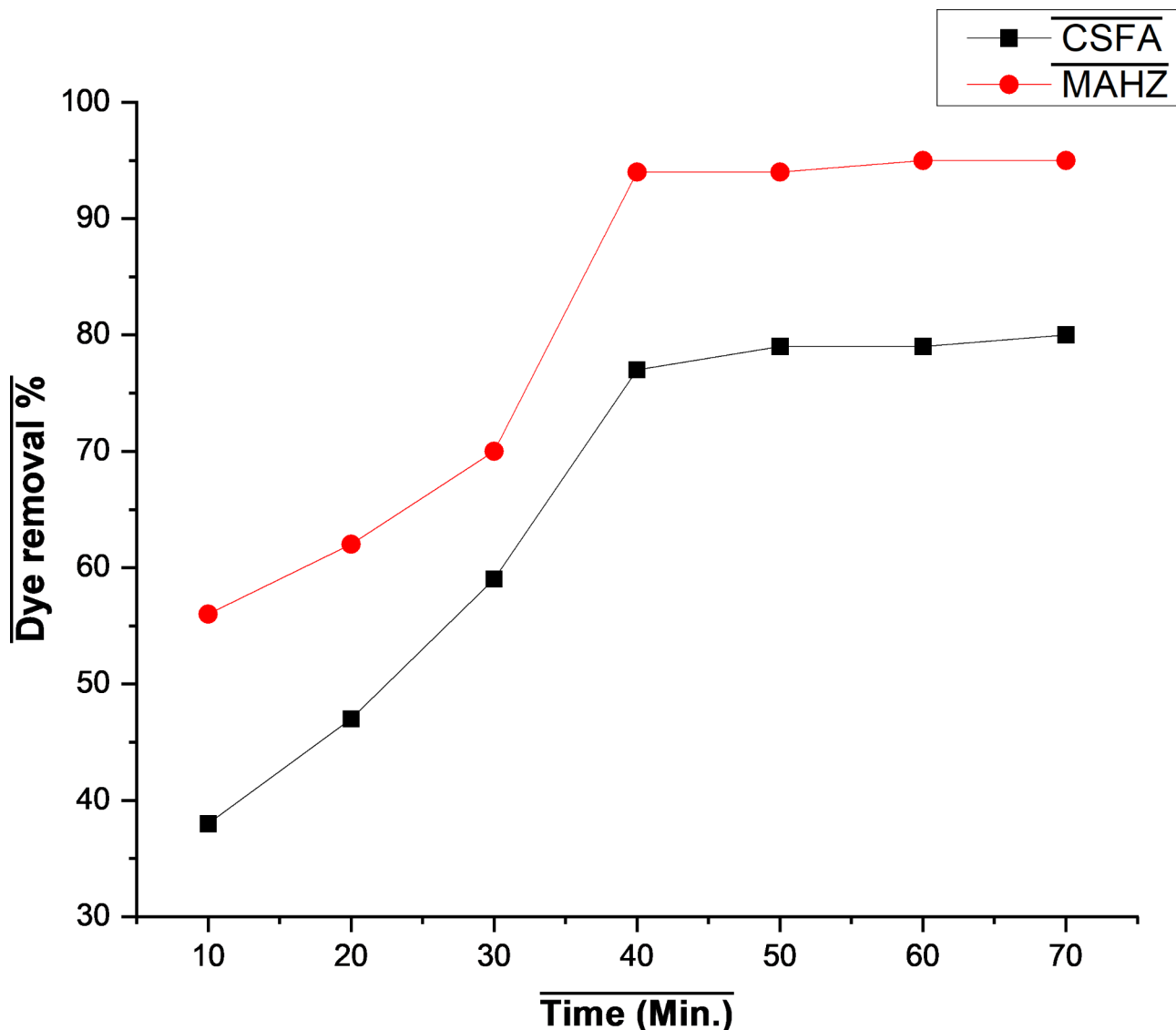


**Fig. 8.** Effect of time on the removal efficiency of RB 19 dye at pH = 8, adsorbent dose: 2.10 g/100mL, initial dye concentration: 100ppm.

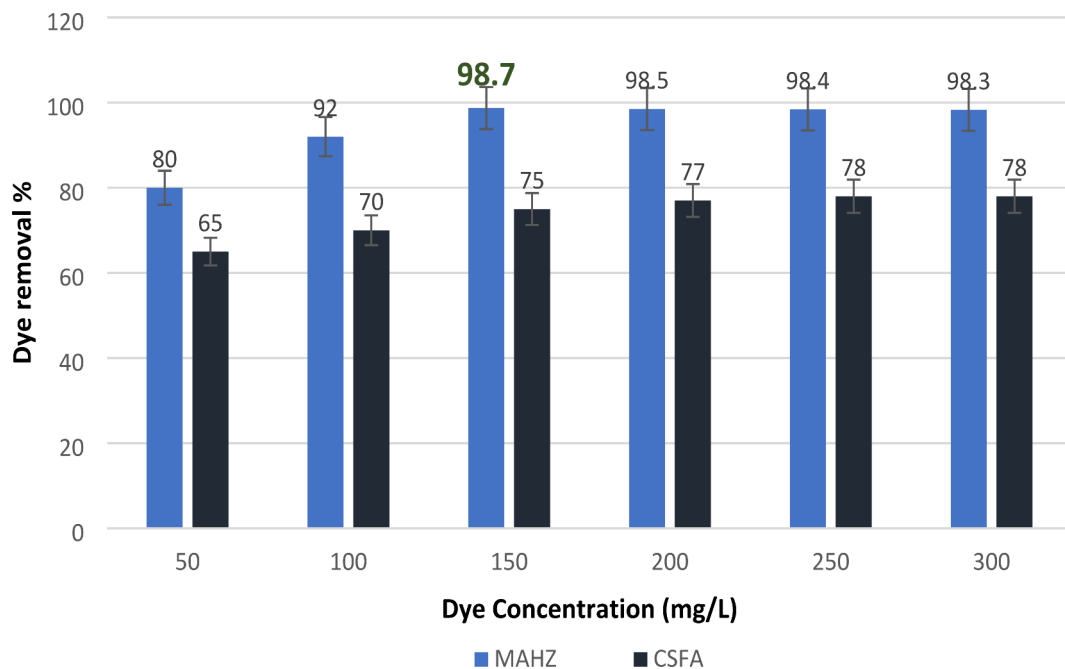


**Fig. 9.** Effect of initial dye concentration on the removal efficiency of RB 19 dye at pH = 8, adsorbent dose: 2.10 g/100mL, time = 40 min.

highlight the adsorption dynamics, data were examined, and experimental results were analyzed with respect to published works. The results are in close agreement with the adsorption studies which are reported in literature<sup>35</sup>.

## Conclusion

The present study demonstrated that corn stem based raw fly ash having 1.112% LOI and 1.411% MC hydrothermally converted into zeolites followed by the comprehensive characterization has revealed many, structural, morphological and other potential aspects of material for potential applications. The utilization of microwave irradiation following the acid treatment of raw material (CSFA) yields great purity, as indicated by the XRD data. Zeolite crystallites deposited on undissolved (CSFA) particles were visible in the SEM micrographs. At pH = 8, MAHZ removed almost 98.7% of the RB 19 dye in 40 min at a dosage of 2.10 g/100 mL. It can be concluded on a logical ground that CSFA based zeolites can be a sustainable approach to recycle the one industrial waste (fly ash) to treat the other waste (wastewater) produced in the industry as a slogan of “zero waste economy” for efficient removal of dyes and other organic and inorganic pollutants. The exploration of further dimensions of this study can open the horizons of repurposing waste or waste to value strategies a way forward to entrepreneurship.

## Data availability

All data generated or analyzed during the study are included in this article.

Received: 17 September 2024; Accepted: 20 January 2025

Published online: 08 May 2025

## References

1. Nazeer, M., Tabassum, U. & Alam, S. Environmental pollution and sustainable development in developing countries. *Pakistan Dev. Rev.*, 589–604 (2016).
2. Ukaogo, P. O., Ewuzie, U. & Onwuka, C. V. Environmental pollution: Causes, effects, and the remedies. In *Microorganisms for Sustainable Environment and Health* 419–429 (Elsevier, 2020).
3. Chatha, S. A. et al. Investigation of the potential of microbial stripping of dyed cotton fabric using white rot fungi. *Text. Res. J.* **81**(17), 1762–1771 (2011).
4. Chatha, S. A. S. et al. Biological color stripping: A novel technology for removal of dye from cellulose fibers. *Carbohydr. Polym.* **87**(2), 1476–1481 (2012).
5. Hussain, M. et al. Application of chitosan-Acacia nilotica bio-composite for wastewater treatment and significance of RSM-model for parametric optimization. *Int. J. Environ. Sci. Technol.* **20**(7), 7487–7500 (2023).
6. Mehmood, S., Reddy, B. V. & Rosen, M. A. Energy analysis of a biomass co-firing based pulverized coal power generation system. *Sustainability* **4**(4), 462–490 (2012).
7. Al-dahri, T., AbdulRazak, A. A. & Rohani, S. Preparation and characterization of Linde-type A zeolite (LTA) from coal fly ash by microwave-assisted synthesis method: Its application as adsorbent for removal of anionic dyes. *Int. J. Coal Prep. Util.* **42**(7), 2064–2077 (2022).
8. Fukasawa, T. et al. Synthesis of zeolite from coal fly ash by microwave hydrothermal treatment with pulverization process. *Adv. Powder Technol.* **28**(3), 798–804 (2017).

9. Musyoka, N. M. et al. Synthesis of templated carbons starting from clay and clay-derived zeolites for hydrogen storage applications. *Int. J. Energy Res.* **39**(4), 494–503 (2015).
10. Miao, Q. et al. Decomposition of the potassic rocks by sub-molten salt method and synthesis of low silica X zeolite. *Asia Pacific J. Chem. Eng.* **11**(4), 558–566 (2016).
11. Lam, S. S. et al. Microwave-assisted pyrolysis with chemical activation, an innovative method to convert orange peel into activated carbon with improved properties as dye adsorbent. *J. Clean. Prod.* **162**, 1376–1387 (2017).
12. Bukhari, S. S. et al. Conversion of coal fly ash to zeolite utilizing microwave and ultrasound energies: A review. *Fuel* **140**, 250–266 (2015).
13. Kisku, G. et al. Characterization and adsorptive capacity of coal fly ash from aqueous solutions of disperse blue and disperse orange dyes. *Environ. Earth Sci.* **74**, 1125–1135 (2015).
14. Jaafari, J. et al. Effective adsorptive removal of reactive dyes by magnetic chitosan nanoparticles: kinetic, isothermal studies and response surface methodology. *Int. J. Biol. Macromol.* **164**, 344–355 (2020).
15. AbdulRazak, A. A., Shakor, Z. M. & Rohani, S. Optimizing Biebrich Scarlet removal from water by magnetic zeolite 13X using response surface method. *J. Environ. Chem. Eng.* **6**(5), 6175–6183 (2018).
16. Majid, Z., AbdulRazak, A. A. & Noori, W. A. H. Modification of zeolite by magnetic nanoparticles for organic dye removal. *Arab. J. Sci. Eng.* **44**, 5457–5474 (2019).
17. Al-Dahri, T. et al. Response surface modeling of the removal of methyl orange dye from its aqueous solution using two types of zeolite synthesized from coal fly ash. *Mater. Express.* **8** (3), 234–244 (2018).
18. Duta, A. & Visa, M. Simultaneous removal of two industrial dyes by adsorption and photocatalysis on a fly-ash-TiO<sub>2</sub> composite. *J. Photochem. Photobiol. a* **306**, 21–30 (2015).
19. Panek, R. et al. Comparison of physicochemical properties of fly ash precursor, Na-P1 (C) zeolite–carbon composite and Na-P1 zeolite—adsorption affinity to divalent pb and zn cations. *Materials* **14**(11), 3018 (2021).
20. Tran, V. A., Kadam, A. N. & Lee, S. W. Adsorption-assisted photocatalytic degradation of methyl orange dye by zeolite-imidazole-framework-derived nanoparticles. *J. Alloys Compd.* **835**, 155414 (2020).
21. Kaladharan, G., Gholizadeh-Vayghan, A. & Rajabipour, F. Review, Sampling, and evaluation of Landfilled fly Ash. *ACI Mater. J.* **116**(4), (2019).
22. Gray, M. L. et al. Physical cleaning of high carbon fly ash. *Fuel Process. Technol.* **76**(1), 11–21 (2002).
23. Lusiba, S., Odhiambo, J. & Ogola, J. Effect of biochar and phosphorus fertilizer application on soil fertility: Soil physical and chemical properties. *Arch. Agron. Soil. Sci.* **63**(4), 477–490 (2017).
24. Gayatri, R. et al. Preparation and characterization of ZnO-zeolite nanocomposite for photocatalytic degradation by ultraviolet light. *J. Ecol. Eng.* **22**(2), 178–186 (2021).
25. Arifin, N. et al. An improved hybrid nanocomposites of rice husk derived graphene (GRHA)/zeolitic imidazolate framework-8 for hydrogen adsorption. *Int. J. Hydrg. Energy* **46**(48), 24864–24876 (2021).
26. Lam, S. S. et al. Fruit waste as feedstock for recovery by pyrolysis technique. *Int. Biodeterior. Biodegrad.* **113**, 325–333 (2016).
27. Bajuk-Bogdanović, D. et al. 12-Tungstophosphoric acid/BEA zeolite composites—characterization and application for pesticide removal. *Mater. Sci. Eng.: B* **225**, 60–67 (2017).
28. Liew, R. K. et al. Microwave pyrolysis with KOH/NaOH mixture activation: a new approach to produce micro-mesoporous activated carbon for textile dye adsorption. *Bioresour. Technol.* **266**, 1–10 (2018).
29. Akar, G. et al. Leaching behavior of selected trace elements in coal fly ash samples from Yenikoy coal-fired power plants. *Fuel Process. Technol.* **104**, 50–56 (2012).
30. Sivalingam, S. et al. Efficient sono-sorptive elimination of methylene blue by fly ash-derived nano-zeolite X: Process optimization, isotherm and kinetic studies. *J. Clean. Prod.* **208**, 1241–1254 (2019).
31. Rafique, M. et al. Characterization and recycling of raw fly ash derived through stems of Sesamum indicum as a proficient adsorbent for chlorazol black E from wastewater. *Kuwait J. Sci.* **50** (4), 602–608 (2023).
32. Hussain, T. et al. Ultrasonic Powered Hydrothermal modification of coal fly Ash to cost-effective zeolites. *J. Chem. Soc. Pak.* **43**(4), (2021).
33. Hussain, S. M. et al. Emerging aspects of photo-catalysts (TiO<sub>2</sub> & ZnO) doped zeolites and advanced oxidation processes for degradation of azo dyes: A review. *Curr. Anal. Chem.* **17** (1), 82–97 (2021).
34. Nadeem, N. et al. Coal fly ash-based copper ferrite nanocomposites as potential heterogeneous photocatalysts for wastewater remediation. *Appl. Surf. Sci.* **565150542** (2021).
35. Fukui, K. et al. Effects of microwave irradiation on the crystalline phase of zeolite synthesized from fly ash by hydrothermal treatment. *Adv. Powder Technol.* **18**(4), 381–393 (2007).
36. Spiekermann, G. et al. Vibrational mode frequencies of silica species in SiO<sub>2</sub>-H<sub>2</sub>O liquids and glasses from ab initio molecular dynamics. *J. Chem. Phys.* **136**(15), (2012).
37. Dogaroglu, Z. G. et al. Synthesis, characterization and optimization of PVA/SA hydrogel functionalized with zeolite (clinoptilolite): Efficient and rapid color removal from complex textile effluents. *Mater. Chem. Phys.* **295**, 127090 (2023).
38. Zhou, Q. et al. Synthesis of high-quality NaP1 zeolite from municipal solid waste incineration fly ash by microwave-assisted hydrothermal method and its adsorption capacity. *Sci. Total Environ.*, 855158741 (2023).
39. Imessaoudene, A. et al. Adsorption performance of zeolite for the removal of Congo red dye: Factorial design experiments, kinetic, and equilibrium studies. *Separations* **10**(1), 57 (2023).
40. Sayed Ahmed, S. A., Khalil, L. B. & El-Nabarawy, T. Removal of reactive blue 19 dye from aqueous solution using natural and modified orange peel. *Carbon Lett.* **13**(4), 212–220 (2012).

## Acknowledgements

The authors are grateful for the financial support from the Government College University, Faisalabad. The authors acknowledge and extend their appreciation to the Researchers Supporting Project Number (RSP-D2025R1005), King Saud University, Riyadh, Saudi Arabia.

## Author contributions

S.S.: Performed the design of the experiment, Formal analysis, carried out the experiment writing—review and editing, original drafted the manuscript. M.S.: Conceptualization, writing—review and editing, funding acquisition. S.A.S.C., S.A. and P.K.S.: Supervision, conceptualization, resources, funding acquisition, writing—review and editing.

## Funding

The authors would like to extend their sincere appreciation to the Government College University, Faisalabad and this work was also funded by the Researchers Supporting Project Number (RSPD2025R1005), King Saud University, Riyadh, Saudi Arabia.

## Declarations

### Competing interests

The authors declare no competing interests.

### Additional information

**Correspondence** and requests for materials should be addressed to S.A.S.C., S.A. or P.K.S.

**Reprints and permissions information** is available at [www.nature.com/reprints](http://www.nature.com/reprints).

**Publisher's note** Springer Nature remains neutral with regard to jurisdictional claims in published maps and institutional affiliations.

**Open Access** This article is licensed under a Creative Commons Attribution-NonCommercial-NoDerivatives 4.0 International License, which permits any non-commercial use, sharing, distribution and reproduction in any medium or format, as long as you give appropriate credit to the original author(s) and the source, provide a link to the Creative Commons licence, and indicate if you modified the licensed material. You do not have permission under this licence to share adapted material derived from this article or parts of it. The images or other third party material in this article are included in the article's Creative Commons licence, unless indicated otherwise in a credit line to the material. If material is not included in the article's Creative Commons licence and your intended use is not permitted by statutory regulation or exceeds the permitted use, you will need to obtain permission directly from the copyright holder. To view a copy of this licence, visit <http://creativecommons.org/licenses/by-nc-nd/4.0/>.

© The Author(s) 2025